Estimating the Volume of Non-Polar Ice on Mars: Geometric Constraints on Concentric Crater Fill (CCF) Along the Martian Dichotomy Boundary

Joe Levy[1], Caleb Fassett[2], and Jim Head[3] [1] University of Texas Institute for Geophysics, Austin, TX, 78758, [2] Mount Holyoke College, South Hadley, MA, 01075, [3] Brown University, Providence, RI 02906. joe.levy@utexas.edu

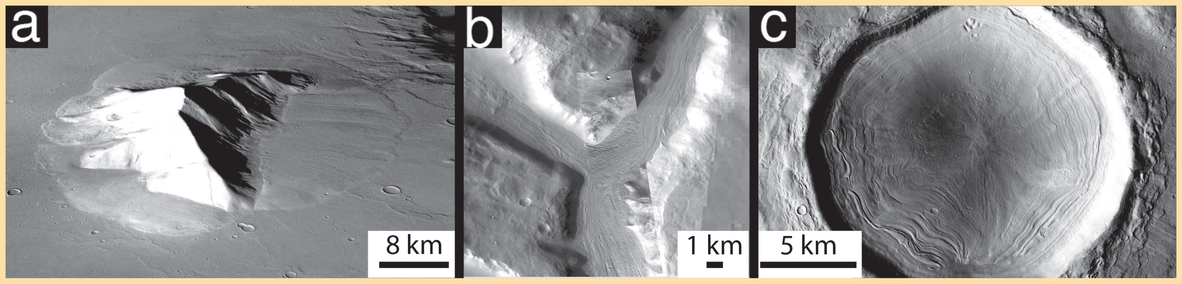

1. Introduction. How much non-polar ice is there on Mars? What is the volume of ice in non-polar, ice-rich surface deposits, and what proportion of the martian water inventory do they represent? To answer these questions, numerous geomorphic analyses have mapped the distribution and age of mid-latitude landforms interpreted as indicators of ground ice in the martian subsurface [1-13]. (a) LDA (b) LVF (c) CCF.

Here we present a new approach to estimating the volume of CCF deposits on Mars, based on MOLA-derived martian crater depth/diameter/ profile relationships.

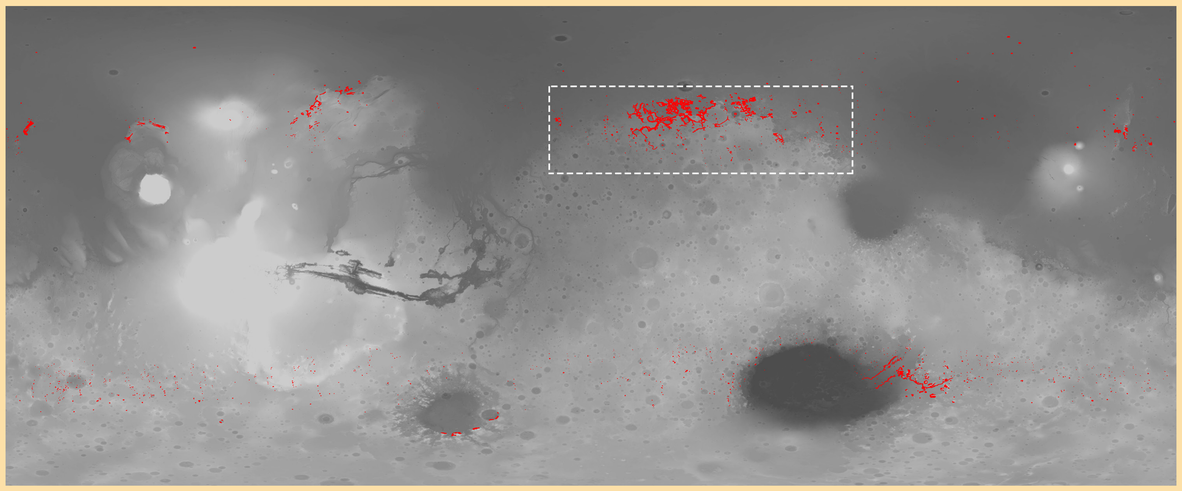

2. Study Area. Map of CCF, LDA, and LVF on mid-latitude Mars identified at 1:500k scale, using CTX image data supplemented by THEMIS. Red features are all glacial landforms. Total LVF/ CCF/LDA area: 4.2 x 10^5 km^2. White box shows area analyzed in detail in this study.

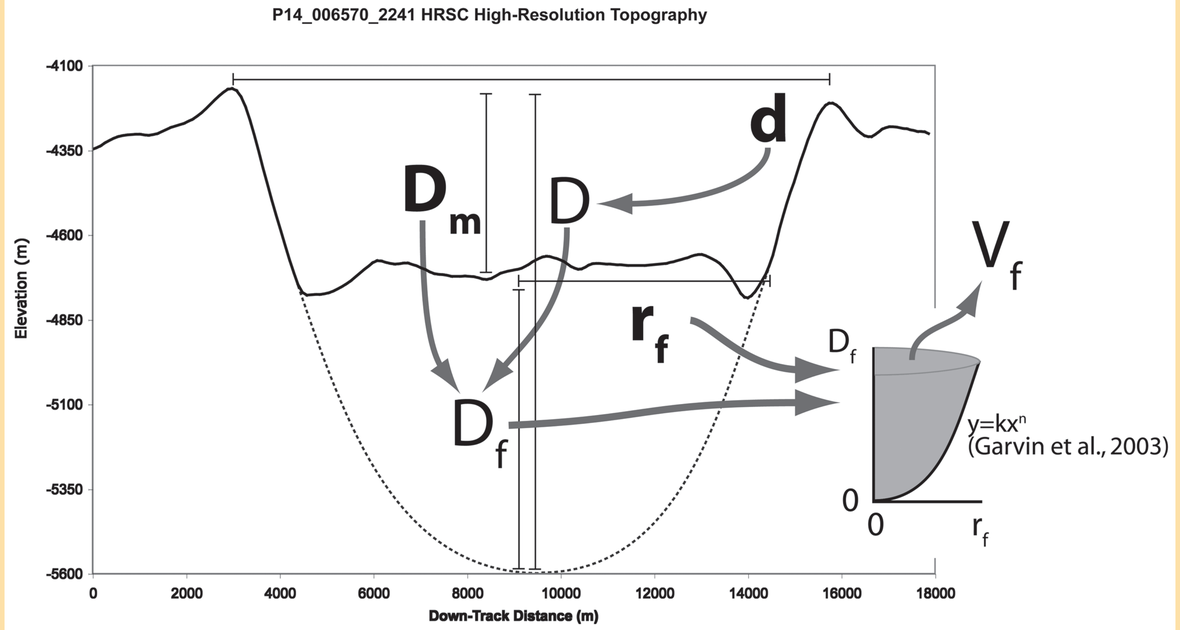

3. Methodology. Several morphometric properties were measured using CTX image data and MOLA gridded topography data for craters containing CCF: crater diameter, d, measured crater depth, D_m, and CCF fill radius, r_f. Diameter, d, is measured as the average rim-to-rim distance from two orthogonal profiles or from the [14] catalog. D_m was measured as the average MOLA elevation of the CCF deposit extracted from two orthogonal profiles or from [14]. r_f, half the diameter of the CCF deposit, was measured using CTX image data measured along two orthogonal profiles that span the spatial limit of "brain terrain" surface texture or concentric surface lineations (geomorphic hallmarks of CCF deposits [13].

Elementary calculus (solids of rotation), permit us to make quantitative estimates of CCF fill volume. The functional relationship between crater diameter (d) and crater depth (D) and crater slope was quantified by Garvin et al. [15]: $d = wD^y$, where w and y are constants that depend on d (all constants reported by [15] vary as a function of d for simple craters, 1-7 km in diameter, complex craters, 7-100 km in diameter, or large craters, >100 km in diameter). The topographic profile of a crater wall follows a similar power-law relationship: here, in Cartesian coordinates of height (y) and radial distance (x): $y = kx^n$ (again, with k and n depending on d) [15].

And, an update on Water Tracks/RSL

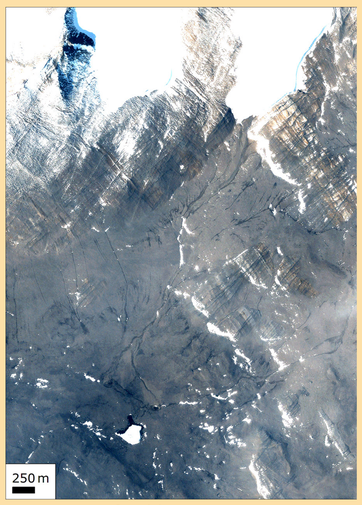

VW2 image of Goldman Basin, Antarctica. January, 2010. Note dark water tracks.

The head wall of a water track. Note that it "emerges" from the bedrock and talus slope.

Using a Geonics EM-38 EM induction probe, it is possible to map soil conductivity (salinity). Water tracks become increasingly saline downslope.

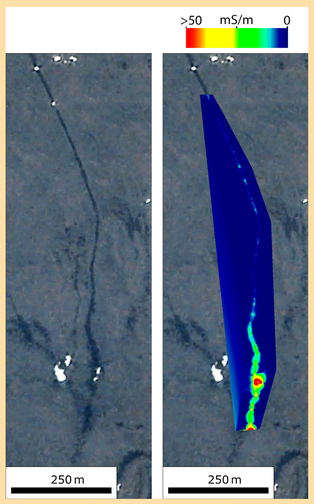

Example Data

Diameter (km)	Max Depth (m)	Model Depth (km)	Fill Thickness (km)	Fill Radius (km)	Fill Volume (km^3)
10.1	90	1.1	1.0	4.5	71
65.6	2250	2.8	0.5	27.5	24
55.0	2500	2.6	0.1	25.0	1
24.2	410	1.7	1.3	10.0	109
48.1	2100	2.4	0.3	23.2	8
45.4	1710	2.3	0.6	19.4	30
42.2	1860	2.3	0.4	15.3	13
41.0	1960	2.2	0.3	18.6	6
40.9	530	2.2	1.7	17.5	172
40.5	1850	2.2	0.4	18.3	11

4. Results. CCF ice volume calculations for this small portion of the martian surface range from 1.2 x 10^4 km^3 to a maximum of 3.7 x 10^4 km^3 (assuming rock-glacier ice mixing ratios and debris-covered glacier ice mixing ratios, respectively). Extrapolating these values to mid-latitude CCF-bearing regions outside of the study area, yields planet-wide CCF ice volumes spanning from 6.0 x 10^4 km^3 to 2.0 x 10^5 km^3.

Support from NASA MDAP Award NNX12AJ46G to JSL, CIF, & JWH.

References: [1] R.P. Sharp R (1973), JGR, , 78, 4073–4083. [2] S.W. Squyres S.W. (1978) Icarus, 34, 600–613. [3] S.W. Squyres SW. (1979), JGR, 84, 8087-8096 [4] S.W. Squyres & M.H. Carr (1986) Science 231, 249–252. [5] B.K. Lucchitta (1984) LPSC, B409–418. [6] V.R. Baker et al. (1991) Nature, 352, 589–594. [7] A. Colaprete & B.M. Jakosky BM (1998) JGR, 103, 5897–5909. [8] N. Mangold (2003) JGR, 108, doi:10.1029/2002JE001885. [9] T.L. Pierce & D.A. Crown (2003) Icarus, 163, 46–65. [10] H. LI et al. (2005) Icarus, 176, 382–394. [11] J.W. Head et al. (2006) EPSL, 241, 663–671. [12] J.W. Head et al. (2006) GRL, 33, doi:10.1029/2005GL024360. [13] J.S. Levy et al. (2010) Icarus, 209, 390–404. [14] Boyce, J.M. et al. (2005) JGR, 110, doi:10.1029/2004JE002328 [15] J.B. Garvin et al. (2001) 6th Mars, Abstr. #3277.